Clim Dyn (2012) 38:547–562
DOI 10.1007/s00382-010-0957-1

Changma onset definition in Korea using the available water resources index and its relation to the Antarctic oscillation

Ki-Seon Choi · Bin Wang · Do-Woo Kim

Received: 1 August 2010 / Accepted: 23 November 2010 / Published online: 19 December 2010

Abstract This study defines the Changma onset using the available water resources index (AWRI) for 25 years (1985–2009) and verifies the validity of this definition. The three conditions for defining the Changma onset are established as follows: (i) The first day exceeding the June AWRI (threshold) averaged over the 25-year period. (ii) The continuation of the value over the threshold for at least 1 week after the onset. (iii) After the continuation of more than 1 week, the non-continuation of the value under the threshold for at least 1 week. The 25-year average Changma onset date is 24 June with a standard deviation of 9 days. The defined Changma onset is verified through the analysis on the relationship with the Antarctic oscillation (AAO). AAO in June shows a high correlation with not only the Changma onset but also the June precipitation (AWRI) in Korea. These three variables are influenced by Mascarene and Australian (positive AAO pattern) highs from in the preceding March. When these two pressure systems develop, the cold cross-equatorial flow in the direction from the region around Australia to the equator is intensified, which in turn, forces a western North Pacific high (WNPH) to develop northward; this eventually drives the rain belt north. As a result, the Changma begins early in the positive AAO phase, and the June precipitation increases in Korea. In addition, a WNPH that develops more northward increases the landfalling frequency of tropical cyclones in Korea, which plays an important role in increasing the June precipitation.

Keywords Available water resources index · Antarctic oscillation · Changma · Mascarene high · Australian high · Tropical cyclone

1 Introduction

The rainy season in Korea can generally be categorized into three periods; the spring rainy period (early April–mid May), Changma (late June–late July), and second Changma or Kaul-Changma (Hereafter, second Changma, mid August–early September) (Byun and Lee 2002). The precipitation during the Changma accounts for more than half of the annual precipitation. Thus, June, which is when Changma begins, is an important month in terms of the variation in the annual precipitation, and shifts in the Changma onset date are a significant concern.

Studies in Korea continue to be carried out to define the Changma onset. In the past, the Changma onset was determined on the basis of when the Changma front lands; it would then be evaluated in terms of which region the front affects and from how much and how long rain falls (Kim 1979; Kim et al. 1983). However, this method of using precipitation to determine the Changma onset overlooked the fact that precipitation in the summer is heavily influenced by Korea's topography. In addition, determining the Changma onset by using the passage of the Changma front around Korea according to weather charts can bring the analyst's subjectivity into play. Recently, there have

K.-S. Choi (✉)
National Typhoon Center/Korea Meteorological Administration, Jeju, Korea
e-mail: choiks@kma.go.kr

B. Wang
Department of Meteorology, International Pacific Research Center, University of Hawaii at Manoa, Honolulu, HI, USA

D.-W. Kim
Department of Environmental Atmospheric Sciences, Pukyong National University, Busan, Korea

been attempts to define the Changma onset objectively. Byun and Lee (2002) developed the water available resource index (AWRI) using precipitation observed by the Korea Meteorological Administration (KMA) and defined the hydrometeorological Changma onset and withdrawal dates using AWRI. Ha et al. (2005) also defined the Changma onset as the date from when precipitation more than the average maximum for the spring rainy period continues for more than 3 days, and simultaneously, the insolation decreases and the relative humidity is over 75% or the total cloud amount is over 70%. When the above conditions are insufficient for determining the Changma onset, they defined it as the beginning point of the increase in the southerly before reaching its maximum value. However, having to consider many climate factors to determine Changma onset is inconvenient. Thus, defining the Changma onset date according to these methods is not still insufficient.

The East Asian summer monsoon (EASM) is an important element in the Asian climate system and is characterized by very complex spatiotemporal features due to its location between the tropics (or subtropics) and polar regions (Lau and Li 1984; Tao and Chen 1987). There have been efforts to determine the causes for variations in the EASM caused by various climate factors. For studies on the relation with the El Niño-Southern oscillation (ENSO), Ha et al. (2005) indicated that the Changma onset date is closely related to Niño-4 SST in the preceding spring, and Huang and Wu (1989) showed that the precipitation in eastern China increases considerably for the next summer after El Niño. Chang et al. (2000) also demonstrated that the precipitation in May and June in Yangtze River valley is strongly influenced by warm SST in the equatorial eastern Pacific for the preceding winter. However, they could not explain the clear physical mechanism on the lag-correlation between EASM and climate factors.

There have been several studies on the relation with Arctic oscillation (AO). Gong and Ho (2003) proved that the anomalous sinking motion is intensified in Japan from the Yangtze River valley because the summer upper tropospheric jet stream shifts northward in East Asia in the preceding spring positive AO phase; consequently, the atmospheric conditions get drier in the summer in this region. As for more recent studies, Ju et al. (2005) showed that the summer precipitation in Korea from northeastern China has increased due to the strengthening of the positive AO phase in the preceding winter since the late 1970s. They suggested that the weakening of a western North Pacific (WNP) high (WNPH) by the strengthening of AO is the cause of the decreasing precipitation in these regions.

There have also been studies on the relation between the East Asian Jet (EAJ) and EASM. As a pioneer study, Yeh et al. (1959) mentioned that the meridional displacement of the EAJ is the reliable indicator of the EASM onset and retreat. Since then, studies have shown that the EAJ has a position identical to that of rain bands such as Mei-Yu or "plum rains" (Tao and Chen 1987; Lau et al. 1988; Ding 1992). More recently, Liang and Wang (1998) showed that the poleward (equatorward) shift of the summer EAJ generates more precipitation than average in northern (central and southern) China; they then demonstrated their results using a general circulation model.

There have also been several efforts to relate EASM to the circulation system in the Southern Hemisphere (SH). Antarctic oscillation (AAO) is a typical annular mode circulation distinct in the SH during the boreal summer or austral winter. It primarily features a large-scale seesaw oscillation of atmospheric circulation between the mid-latitudes and high-latitudes in the SH (Kidson 1988; Gong and Wang 1999; Thompson and Wallace 2000). This AAO is known to influence various climate variations in the SH including total column ozone, tropopause heights in the mid-latitudes and high-latitudes, and intensity of trade wind (Thompson and Wallace 2000); variations in sea ice, sea surface temperature, and Antarctic surface air temperature (Hall and Visbeck 2002; Kwok and Comiso 2002); variations in precipitation in southeastern South Africa, western South Africa, and Australian (Silvestri and Vera 2003; Reason and Rouault 2005; Hendon et al. 2007). The AAO also influences climate variation in the summer in the Northern Hemisphere (NH) through teleconnection pattern. Ho et al. (2005) showed that the huge Australian high (AH), which is located around Australia in the positive AAO phase, intensifies cross-equatorial flows, which, in turn, dives the WNPH to develop in the mid-latitudes of East Asia, and eventually, the tropical cyclone (TC) activity also increases in these regions. Wang and Fan (2007) stressed that the TC genesis frequency becomes lower than average in the positive AAO phase because convection is only active in the region around the equator. WNPH that has intensified in the positive AAO phase in the mid-latitudes region of East Asia is also known to play a role in reducing the dust frequency in northern China (Fan and Wang 2004). However, studies on the relation between AAO and EASM have only focused on the variation in precipitation over the Yangtze River valley (Gao et al. 2003; Xue et al. 2004; Wang and Fan 2005; Fan 2006; Sun et al. 2009). The commonality of these studies is that the intensified AH in the positive AAO phase plays a role as a bridge between AAO in the SH and EASM in East Asia. In particular, these studies have shown that since AH is clearly observed from the preceding spring, it can be used as a predictor for EASM.

In this study, we first define the Changma onset from 1985 to 2009 using AWRI. We use data after 1985 because previous studies have shown that TC activity and sunshine

duration, including EASM, have changed considerably since the early or mid 1980s (Sato and Takahashi 2001; Inoue and Matsumoto 2003, 2007). The validity of the defined Changma onset is then verified through the correlation analysis with AAO.

The data and definitions are presented in Sect. 2, and the Changma onset in Korea is defined in Sect. 3. The relation between the Changma onset and AAO in June is discussed in Sect. 4, and the validity of the Changma onset through analysis of the difference between high and low AAO years is verified in Sect. 5. In Sect. 6, the relation between the preceding spring AAO and the Changma onset is examined to evaluate a predictor for the prediction of Changma onset. This study is summarized in Sect. 7.

2 Data and definitions

2.1 Data

2.1.1 Reanalysis data

We use 25 years (1985–2009) of data on geopotential height (gpm), horizontal wind (m s^{-1}), vertical velocity (hPa s^{-1}), and specific humidity (g kg^{-1}) that are reanalyzed by the National Centers for Environmental Prediction–National Center for Atmospheric Research (NCEP–NCAR) (Kalnay et al. 1996; Kistler et al. 2001). The NCEP-NCAR reanalysis datasets have a horizontal resolution of 2.5° × 2.5° latitude–longitude with 17 vertical pressure levels (specific humidity has just 8 vertical pressure levels).

The NOAA interpolated outgoing longwave radiation (OLR) data that retrieved from the NOAA satellite series are used. The OLR data is available from June 1974 from the NOAA's Climate Diagnosis Center (CDC). However, there is a missing period for March–December 1978. Detailed information regarding OLR data can be found at the CDC website (http://www.cdc.noaa.gov) or in the paper by Liebmann and Smith (1996).

In addition, Climate Prediction Center Merged Analysis of Precipitation (CMAP) data (Xie and Arkin 1997) is used; the data has a horizontal spatial resolution that is the same as the NCEP-NCAR reanalysis dataset. The data is composed of the monthly and pentad averages and is available from 1979. The CMAP data, which is the global precipitation data that covers the ocean, are derived by merging rain gauge observations, five different satellite estimates, and numerical model outputs.

2.1.2 Tropical cyclone data

Information about TC activity is obtained from the best track archives of the Regional Specialized Meteorological Center (RSMC), Tokyo Typhoon Center. The datasets consist of TC names, longitude and latitude positions, intensity (minimum surface central pressures and maximum sustained wind speed) measured every 6-h for 25 years. TCs are generally divided into four categories based on their maximum sustained wind speed (MSWS); tropical depression (MSWS < 17 m s^{-1}), tropical storm (17 m $s^{-1} \leq$ MSWS ≤ 24 m s^{-1}), severe tropical storm (25 m $s^{-1} \leq$ MSWS ≤ 32 m s^{-1}), and typhoon (MSWS ≥ 33 m s^{-1}). This study focuses on extratropical cyclones (ECs) that extratropically transformed from TCs as well as TCs in these four categories. ECs are included in this study because they cause damage in the mid-latitudes of East Asia.

2.1.3 Observed precipitation data

In this study, the June total precipitation data for 25 years are obtained from 60 weather observation stations of the KMA (Fig. 2). However, we excludes precipitation at the Ullungdo weather observation station because it is an island far away from the Korean Peninsula and thus has a unique climate that behaves differently.

2.2 Definitions

2.2.1 Warm and cold ENSO years

Using the SST anomalies (SSTA) in the Niño-3.4 region (5°S–5°N, 170°W–120°W), warm (SSTA ≥ 0.5°C) and cold (SSTA ≤ 0.5°C) ENSO years are defined. The climatological mean SST for 25 years is used to obtain SSTA.

2.2.2 AAO index

The AAO index can be taken from the leading EOF mode of 850-hPa geopotential height (Thompson and Wallace 2000) or the difference in the normalized zonal mean SLP between 40°S and 65°S (Gong and Wang 1999). This study uses the monthly AAO index provided by the NOAA/National Prediction Center (http://www.cpc.noaa.gov/products/precip/CWlink/daily_ao_index/aao/aao_index.html). The monthly AAO index is constructed by projecting the daily and monthly mean 1,000 or 700-hPa height anomalies poleward of the 20° latitude for the SH onto the leading EOF mode. The time series is normalized by the standard deviation of the monthly index (1979–2000 base period).

2.2.3 Available water resources index

Byun and Lee (2002) used daily precipitation data of KMA's 60 weather observation stations since 1974 to define AWRI. The AWRI is calculated from the value of the accumulated precipitation; the daily reduction of water

(runoff, evapo-transpiration, infiltration, etc.) and the duration of accumulation are taken into account quantitatively. The accumulated precipitation can be calculated by using Eq. 1.

$$E = \sum_{N=1}^{D} \left(\sum_{m=1}^{N} Pm/N \right) \quad (1)$$

where Pm is the daily precipitation of m days before, N is a dummy variable and E is the representative value of water resources accumulated during D days. Equation 1 is derived from the concept that the precipitation of m days before is added to the total of current water resources as a form of average precipitation for m days. The accumulated precipitation calculated by Eq. 1 is then converted to the AWRI by

$$W = E/\left(\sum_{N=1}^{D} 1/N \right) \quad (2)$$

where, W is the AWRI, which acts as a kind of extensive measure to indicate the amount of current water resources. The high value for W indicates that a large amount of water resources are available, and a small value indicates a deficiency. Because W takes into account the daily reduction of water resources after precipitation, it can show daily changes in water-related conditions more effectively than other values or indexes determined using simple accumulated precipitation. More detailed information regarding the daily loss of water resources can be found in the paper by Byun and Lee (2002).

3 Definition of Changma onset

Wang et al. (2004) systematically arranged studies defining the South China Sea summer monsoon (SCSSM) onset. According to them, most studies defining the SCSSM onset tend to use variables relating rainfall (OLR, brightness temperature, high cloud amount, etc.) with zonal or meridional winds. In contrast, Choi and Byun (2007) documented studies defining the EASM onset (see Table 1 in their paper). According to their investigation, the variables which used to define the SCSSM onset are also used to define the EASM onset. Most studies defining the SCSSM and EASM onsets showed in common that once a southerly containing a great quantity of water vapor becomes significant, the precipitation increases and the summer monsoon begins.

In this study, the AWRI is used to define the Changma onset. Using this index, they classified the rainy seasons in Korea into three periods as follows: Bom-Changma (early April–mid May), Changma (late June–late July), and second Changma (mid August–early September). They also defined these three rainy periods as comprising the hydrological summer monsoon season. The rainy seasons defined by this index has a hydrometeorological meaning and reflect the climate in East Asia well from an agricultural perspective, which indicates that this index is advantageous for quantitatively evaluating the amount of water resources available for industrial and the agricultural use. Moreover, they stressed that there need no many variables to define the onsets of the summer monsoon or rainy season. Thus, the Changma onset in this study is defined using AWRI available for the daily life (Fig. 1). The Changma onset date is defined as the date for which the AWRI meets the following three conditions:

(i) Does it exceed the 25-year average June AWRI (167.2 mm)?
(ii) Is the days under the threshold after Changma onset <1 week?
(iii) Although conditions (i) and (ii) are met, do the days under the threshold after Changma onset continue for at least 1 week?

For example, the AWRI exceeds the threshold on June 16, 1986, but it dose not continue for more than 1 week; eventually, the Changma onset date is defined as June 22 (Fig. 1). In contrast, the AWRI exceeds the threshold value on June 2, 1987 and continues for more than 1 week, but after that the days under the threshold continues for more than 1 week (late June–early July). It is only after July 11 that the days over the threshold continue for more than

Table 1 Comparison of Changma onset dates obtained from the previous studies and the present study

Year	Present study	KMA	Ha et al. (2005)
1985	23 Jun	21 Jun	21 Jun
1986	22 Jun	20 Jun	12 Jun
1987	11 Jul	23 Jun	5 Jul
1988	12 Jul	22 Jun	23 Jun
1989	8 Jun	23 Jun	13 Jun
1990	19 Jun	18 Jun	18 Jun
1991	7 Jul	15 Jun	27 Jun
1992	13 Jul	22 Jun	9 Jul
1993	28 Jun	18 Jun	21 Jun
1994	30 Jun	17 Jun	26 Jun
1995	8 Jul	21 Jun	30 Jun
1996	17 Jun	19 Jun	16 Jun
1997	25 Jun	20 Jun	24 Jun
1998	25 Jun	12 Jun	11 Jun
1999	1 Jul	17 Jun	16 Jun
2000	27 Jun	16 Jun	21 Jun
2001	24 Jun	21 Jun	17 Jun
2002	5 Jul	19 Jun	23 Jun
2003	27 Jun	22 Jun	17 Jun
2004	19 Jun	22 Jun	22 Jun

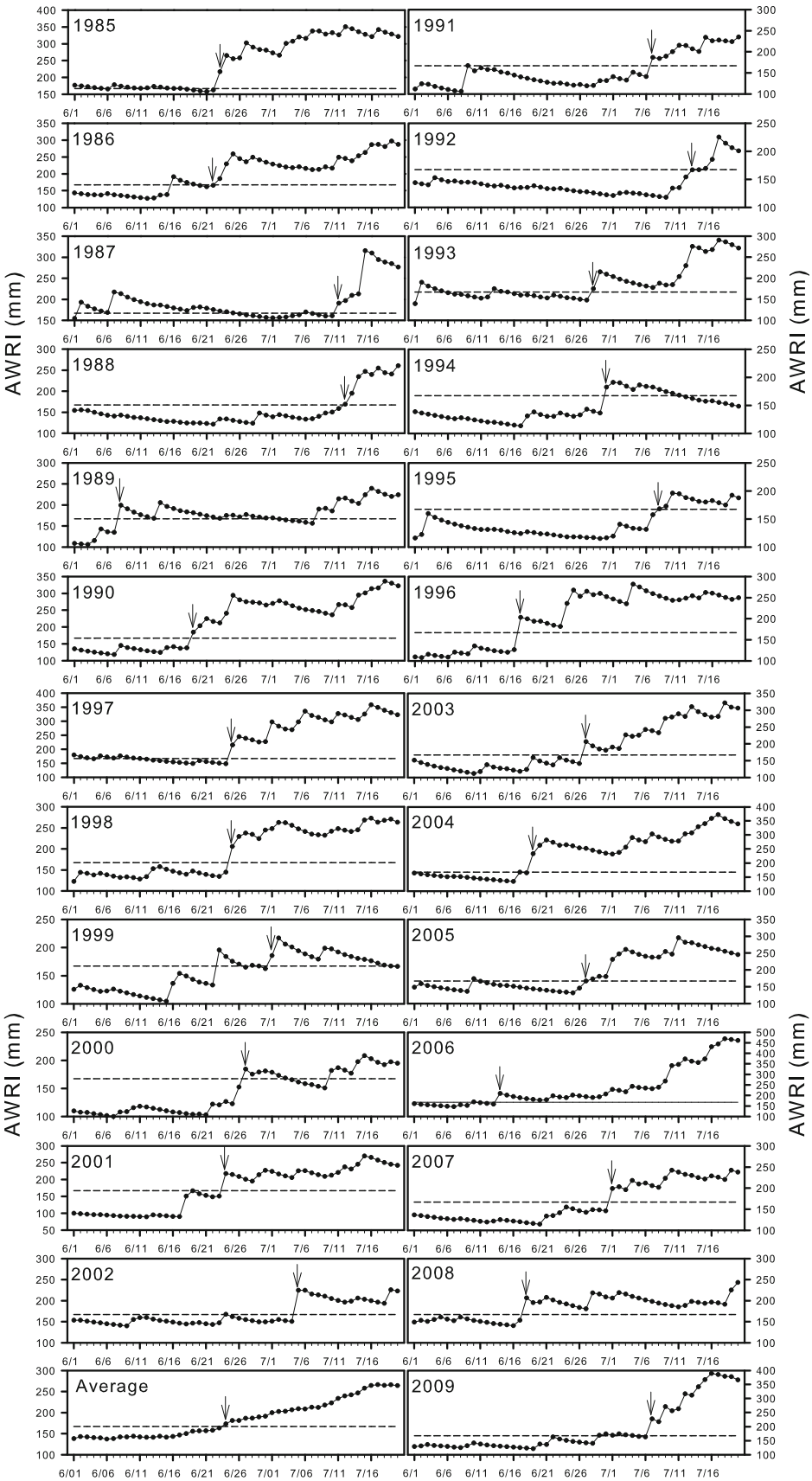

Fig. 1 Changma onset date defined in time series of available water resources index (AWRI) of each year for 25 years. *Arrows* and *dashed lines* denote the Changma onset date and average AWRI in June for 25 years, respectively. Unit is mm

1 week. Therefore, the Changma onset date in 1987 is defined as July 11 rather than June 2. The earliest and the latest Changma onset dates obtained by this process for the 25-year period are June 8, 1989 and July 13, 1992, respectively. The average Changma onset date for 25-year period is June 24 with a standard deviation of 9 days. This date differs little from the Changma onset dates defined in other previous studies (Tao and Chen 1987; Wang and Lin 2002). However, there are some differences compared with Changma onset dates defined by other Korean research (Ha et al. 2005) and KMA (1996). This implies how difficult and complicated it is to define the Changma onset.

This study also applies the definition of the Changma onset to sixty weather observation stations over Korea (Fig. 2). In general, the more northward the region, the later the Changma begins; however, the latest Changma onset is observed in the central eastern region, where it is defined as July 9 at the Uiseong weather observation station (36.36°N, 128.69°E). As illustrated in the embedded map shown in Fig. 2, this characteristic may be due to the terrain effect of the station's location between the Taebaek and Sobaek mountains. However, the exact reason should be determined from the numerical model using high-resolution data. Meanwhile, the earliest Changma onset is observed at the Jeju weather observation station (33.51°N, 126.53°E), which is in the most southern region; the onset is defined as June 13.

4 Correlation between the Changma onset and June AAO

To verify the Changma onset definition of this study, its relationship in June with AAO and precipitation in Korea is examined. The June precipitation shows the strong positive correlation ($r = 0.65$ at the 99% confidence level) with the June AWRI used to define the Changma onset (not shown). However, the relation between these two variables may not be exactly identical due to the consideration of the daily precipitation runoff from the soil when calculating AWRI, as stated above. Therefore, in case that there is a low (high) amount of precipitation in June, AWRI in June can have the high (low) value if the preceding precipitation is high (low).

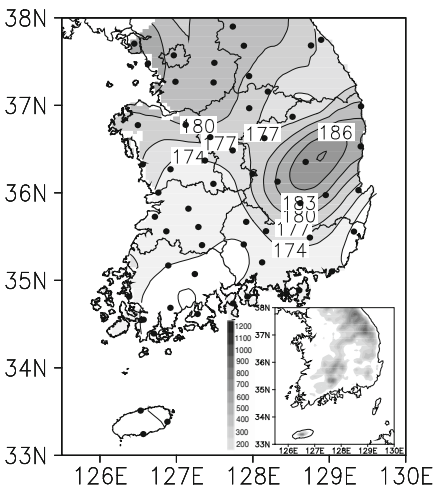

Calendar date		Julian date
June	16	167
	17	168
	18	169
	19	170
	20	171
	21	172
	22	173
	23	174
	24	175
	25	176
	26	177
	27	178
	28	179
	29	180
	30	181
July	1	182
	2	183
	3	184
	4	185
	5	186

Fig. 2 Spatial distribution of the average Changma onset date (Julian date) for 25 years. Contour interval is 3 days. The *right table* is a calendar date corresponding to Julian date

Figure 3 shows the AAO times series in June, the June precipitation in Korea, and the Changma onset date as defined in this study for a 25-year period. There is a strong positive correlation between AAO and precipitation (Fig. 3a). This indicates that if AAO is strong in the SH, the June precipitation in Korea can increase. Although this is consistent with the results of previous studies, it is meaningful in that the direct relation of AAO with June precipitation in Korea is analyzed. A higher negative correlation is found in the relation between AAO and the Changma onset (Fig. 3b). This implies that if AAO is strong in the SH, the Changma can begin early. As a result, a multi-correlation can be established as follows: if AAO in June is intensified, the Changma onset can be advanced; this then causes the June precipitation in Korea to increase (Fig. 3c). All three correlation coefficients are significant at the 99% confidence level.

The correlation between June AAO and precipitation can be further analyzed by expanding the region under study (Fig. 4). First, a positive correlation with AAO in CMAP is distinctly established in the zonal direction from northern China to Korea and Japan (Fig. 4a). In these regions, the relation is highest in Korea ($r = 0.65$ at the 99% confidence level) and northern Japan ($r = 0.74$ at the 99% confidence level). A positive correlation of over 0.5 at the 99% confidence level is also found in the maritime continental region (0°–20°S, 100°–140°E). The OLR shows a correlation contrary to CMAP (Fig. 4b). This indicates that the higher the negative correlation, the higher the possibility of precipitation. The negative correlation is highest in Korea in the mid-latitudes of East Asia, but its correlation coefficient is smaller than that of CMAP. These results indicate that the correlation between the June AAO and precipitation is relatively distinct to Korea.

5 Difference between high AAO years and low AAO years

To understand the possible cause of the high correlation of AAO with the June precipitation in Korea and the Changma onset, the 5 years with the highest AAO (hereafter high AAO years) and the 5 years with the lowest AAO (hereafter low AAO years), excluding warm ENSO years (1987, 1991–1994, 1997, 2002, 2009) and cold ENSO years (1985,

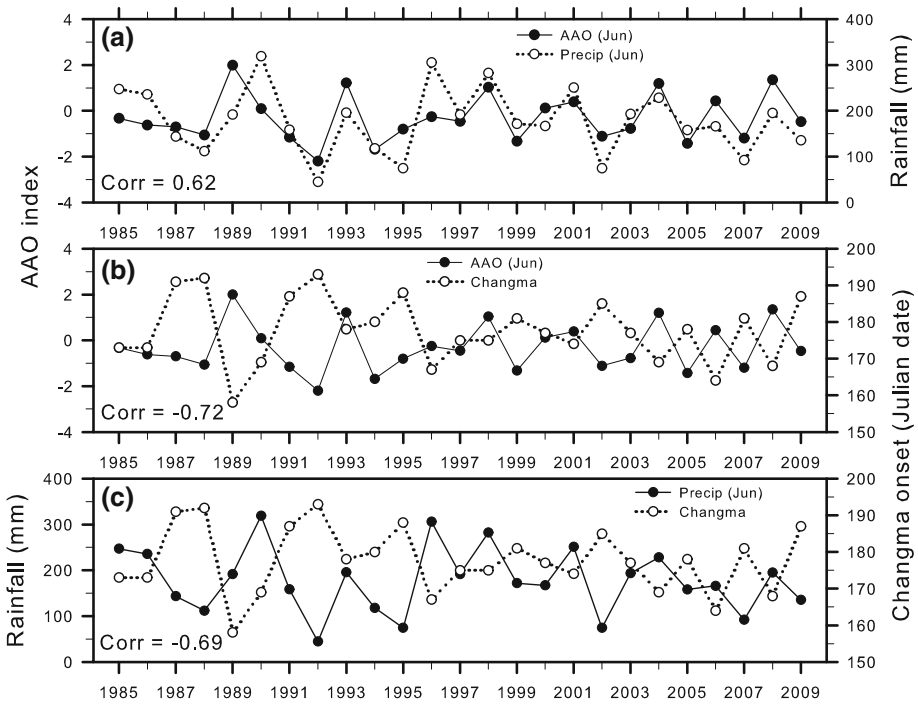

Fig. 3 Time series of Antarctic oscillation (AAO) index and June precipitation in Korea, and Changma onset date

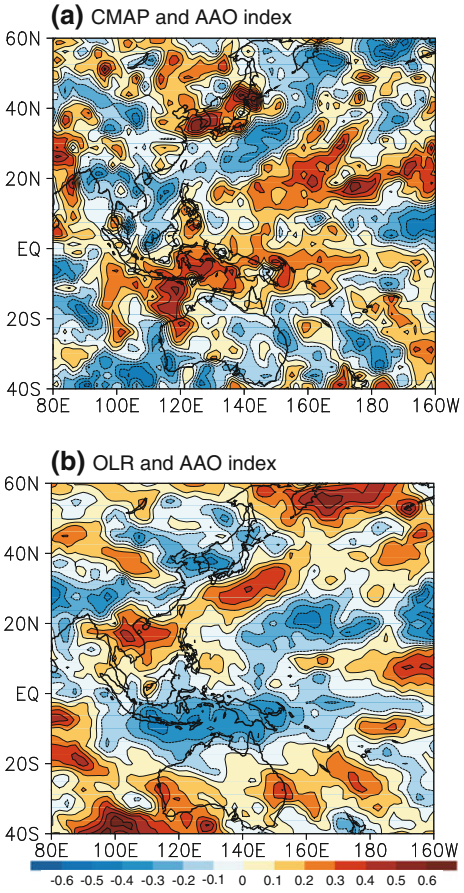

Fig. 4 Correlation distributions between (**a**) CMAP and AAO index in June and (**b**) OLR and AAO index in June. Contour interval is 0.1

1988–1989, 1999, 2000, 2008) in June are selected from the AAO time series for the 25-year period (Table 2). Precipitation in all of the high AAO years except for 2006 exceeds the average precipitation (178.1 mm) for the 25-year period, while in the low AAO years, 3 years (1995, 2005, 2007) have less precipitation than the average. The average June precipitation during the high AAO years is approximately 100 mm greater than in the low AAO years. This corresponds to a precipitation that is 20 mm greater every June during the high AAO years compared to the low AAO year. For AWRI as well, the moderate shortage of water resources is only recorded for 2001 during the high AAO years, while the low AAO years has 3 years with the moderate shortage of water resources. Table 3 presents information regarding the legend for AWRI. The moderate shortage of water resources recorded in the average AWRI for the low AAO years indicates that the water resources available for the agricultural and industrial use are insufficient in June of these years. The average Changma onset date for the 25-year period is June 24; the Changma onset date for the high AAO years is earlier by 5 days, while it is later by 4 days for the low AAO years. In other words, the average Changma onset date is later by 10 days for the low AAO years compared to the high AAO years.

5.1 Spatial distribution of precipitation, AWRI, and Changma onset over Korea

Figures 5 and 6 show the spatial distributions for the precipitation, AWRI, and Changma onset at each weather

Table 2 Statistics of high AAO years and low AAO years defined from the time series in Fig. 1

High AAO years				Low AAO years			
Year	Precip (mm)	AWRI (mm)	Changmaonset	Year	Precip (mm)	AWRI (mm)	Changmaonset
1990	318.9	189.5	19 Jun	1986	235.6	173.2	22 Jun
1998	282.3	170.3	25 Jun	1995	74.4	130.9	8 Jul
2001	251.1	145.6	24 Jun	2003	193.5	144.2	27 Jun
2004	228.2	204.9	19 Jun	2005	158.1	153.8	27 Jun
2006	166.4	189.7	14 Jun	2007	92.0	133.9	1 Jul
Average	249.4	180.0	19 Jun	Average	150.7	147.2	28 Jun

Here, warm and cold ENSO years are excluded in the analysis

Table 3 Water condition corresponding to the AWRI (Byun and Lee 2002)

AWRI (mm)	Condition of the water resources
$100 \leq \text{AWRI} < 150$	Moderate shortage of water
$50 \leq \text{AWRI} < 100$	Severe shortage of water
$\text{AWRI} < 50$	Extreme shortage of water

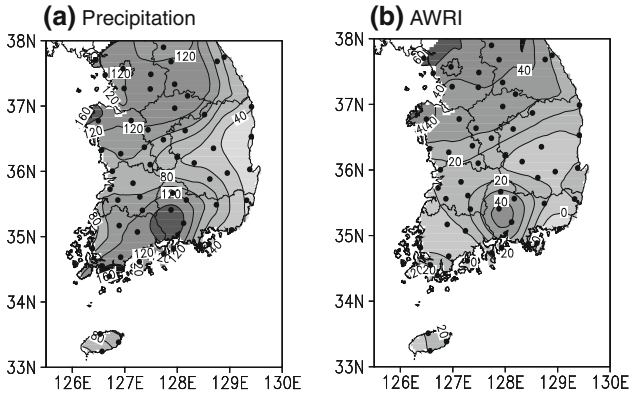

Fig. 5 Difference in the June (**a**) precipitation and (**b**) AWRI between high AAO years and low AAO years. Contour intervals are 20 mm for precipitation and 10 mm for AWRI

observation station; these are analyzed by applying the difference between the two phases. The analysis results for the precipitation and AWRI show that the two variables are higher for all of Korea during the high AAO years (Fig. 5). The largest difference between the two phases is shown in the central area of southern Korea and western area of northern Korea for both variables. Previous studies have showed that because Sobaek mountains is located in the former region, heavy rainfall events have recently increased due to the terrain effect (Seo and Lee 1996; Kim and Lee 2007). The latter region is metropolitan, and the rainfall intensity has greatly increased recently due to increased precipitation caused by the green house effect (Choi 2004; Chang and Kwon 2007).

There is a distinctive difference between the two phases in most regions for the spatial distribution of the Changma onset date (Fig. 6c). The Changma is first characterized as beginning before June 20 in most regions of Korea during the high AAO years except for the central eastern region where Changma has the latest onset date for the 25-year period (Fig. 6a). The more northward a region is located the later the Changma begins during the low AAO years; the onset date is also relatively later in Jeju island (1 July) (Fig. 6b). There is no place that the Changma begins before June 25 except for part of the southern region. This is why the difference between the two phases gets larger as the region is located more northward; this applies to Jeju as well (Fig. 6c). There are some areas in the northern region where the Changma began later up to 15 days later during the low AAO years than during the high AAO years.

5.2 Intraseasonal variation of precipitation in Korea

The intraseasonal variation in precipitation is analyzed to compare conditions between the two phases for seasons other than June (Fig. 7). The 7-day running average precipitation data is used for this analysis.

Climatologically, there exist two peaks in the intraseasonal variation of precipitation in Korea; Changma (late June–late July) and the second Changma (mid August–early September). Both of two peaks are placed within the summer (June–September) (Byun et al. 1992). Typical intraseasonal variation in precipitation is well observed for the low AAO years. However, in the high AAO years, there are five peaks within the summer. In particular, it is remarkable that there exists the short break period (early July) within the Changma period and the Changma break period (mid July–mid August) between Changma and the second Changma is longer than the climatological average period (early August–mid August). Therefore, the frequency of the rains like a localized heavy rainfall in a few

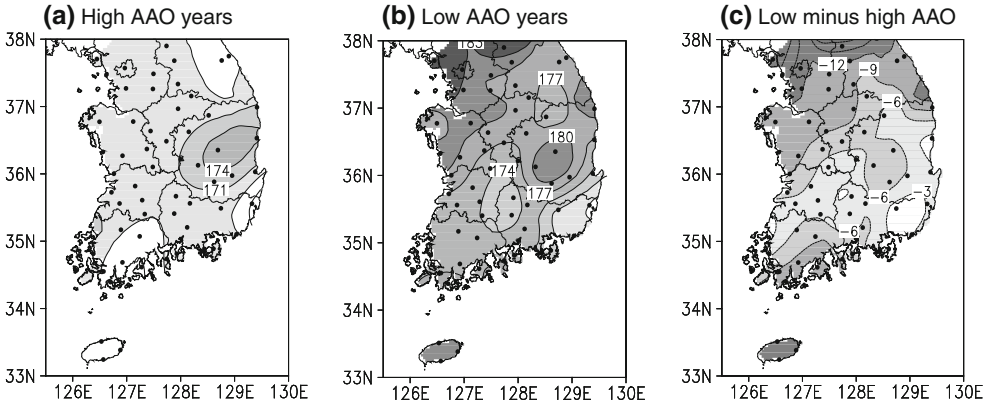

Fig. 6 Changma onset dates for (**a**) high AAO years and (**b**) low AAO years, and (**c**) the difference in the Changma onset date between high AAO years and low AAO years. Contour interval is 3 days. Units are Julian dates for (**a**) and (**b**). Calendar date corresponding to Julian date is shown in Fig. 2

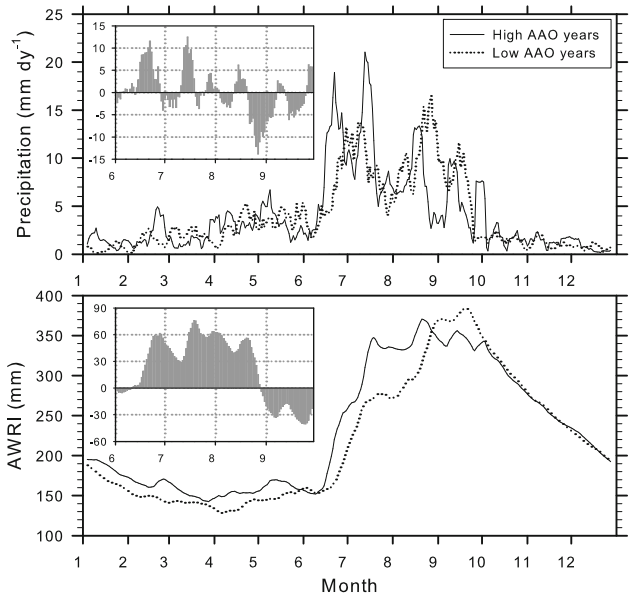

Fig. 7 Temporal variability of the 7-day running average precipitation (*upper*) and AWRI (*lower*) for high AAO years (*solid line*) and low AAO years (*dotted line*). The embedded figures are the difference in precipitation and AWRI for summer (June–September) between high AAO years and low AAO years

hours are likely to be high in the high AAO years. To determine this properly, a more detailed analysis is required using hourly precipitation data. On the other hand, there is a small difference of precipitation of around 4 mm between the two phases for seasons other then the summer. This study examines the difference in precipitation between the two phases during the summer in detailed (embedded map in Fig. 7). The June precipitation is also shown to be higher during the high AAO years. Overall, the 4 months of the summer can be roughly categorized into two sub-periods; more precipitation for June-mid August in the high AAO years and more precipitation for mid August–September in the low AAO years. This implies that in the high AAO years, there is more precipitation during the Changma season before the second Changma season, but in the low AAO years, there is more precipitation since the second Changma season. These characteristics may be related to the Changma onset and withdrawal dates of the two phases (i.e., duration of Changma). In other words, in the high AAO years, the Changma begins and ends early, and more precipitation is recorded in the early summer, the opposite holds true for the low AAO years. Therefore, in the future studies, we plan to define the Changma withdrawal date using AWRI to examine the variability in the summer precipitation between the two phases. For AWRI, the difference between the two phases is clearer. Overall, AWRI is higher in the high AAO years for the period from January to August and in the low AAO years during September. There is no large difference from October to December. This indicates that the water resources are more abundant in the high AAO years during the spring and summer seasons, which is when they are important for agriculture. The difference between the two phases is the largest during the summer. Thus, this study examines the difference between two phases in the summer in detail. The characteristics in the differences of precipitation between the two phases are shown more clearly by the difference in AWRI, i.e., AWRI is higher before the second Changma season in the high AAO years, and since the second Changma season in the low AAO years.

To investigate the difference in precipitation and Changma onset between the two phases in detail, this study examines the characteristics of the variation in the 5-day average rainfall for June in East Asia using CMAP data (Fig. 8). First, for the high AAO years, the main rain band for June 11–15 stretches from the central region of China to the southern region of Japan; in the low AAO years, it

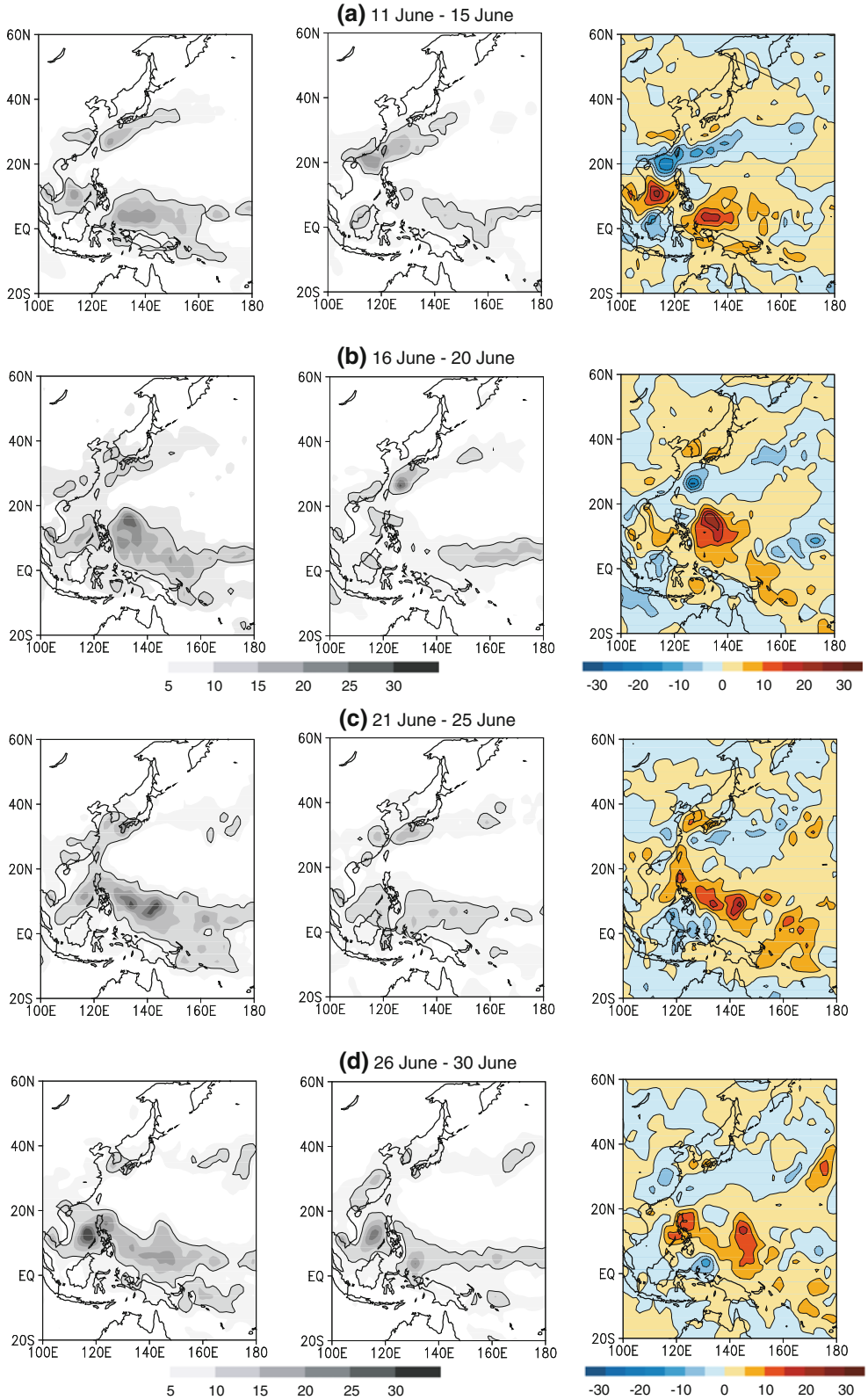

Fig. 8 Time evolution of 5-day average rainfall using the CMAP data during the period from 11 June to 30 June in high AAO years (*left*), low AAO years (middle), and theirs difference (*right*) for 25 years. In the *left* and *middle panels*, contour denotes regions >10 mm day^{-1}

spreads in the southwest-northeast direction from the South China Sea to the sea south of Japan in the lower latitudes (Fig. 8a). For the difference between the two phases, there are more precipitation in the high AAO years with no large differences in Korea. For June 16–20, the main rain band for the low AAO years is located in a similar location as the rain band for June 11–15 in the high AAO years; the main rainfall band in the high AAO years moves more northward, and thus the contour of 10 mm is located in Korea (Fig. 8b). As discussed above, this 5-day period corresponds to the average Changma onset date (June 19) in the high AAO years. As a result, there is the difference in precipitation of more than 10 mm between the two phases in Korea. Many previous studies have suggested a daily precipitation of more than 5–10 mm with a rapid shift of the wind direction signals the summer monsoon onset (Hendon and Liebmann 1990; Wang and Lin 2002; Wang et al. 2004), similar to the threshold of 10 mm used in this study with CMAP data. For June 21–25, the precipitation around Korea in the high AAO years increases and the contour of 15 mm appears; in the low AAO years, the main rain band, which was in the southwest-northeast direction in the preceding 5-day period, becomes more in the zonal direction. However, the contour of 10 mm is still located to the south of Korea. Therefore, there is a large difference of 15 mm in precipitation between the two phases around Korea. For June 26–30, the rain band is a little weakened in the high AAO years compared with the preceding 5-day period (Fig. 8d). As shown in the intraseasonal variation of precipitation in Korea, this indicates that the short break period begins from this point within the duration of the Changma. In the low AAO years, the contour of 10 mm is finally seen in Korea. As analyzed above, the average Changma onset date (June 28) of the low AAO years is located to this 5-day period. The difference between the two phases seems to be decreased in quantity compared with the preceding 5-day period.

5.3 Large-scale atmospheric environments

To determine the cause for the difference in the precipitation and Changma onset between the two phases, this study analyzes the difference between the two phases for the large-scale the atmospheric environments in June.

For the 850-hPa streamline, the anomalous cyclonic circulation in low latitudes under 20°N, the anomalous anticyclonic circulation between 20°–40°N, and the anomalous cyclonic circulation over 40°N in the NH are intensified in the high AAO years (Fig. 9a). The anomalous anticyclone intensified in the mid-latitudes of East Asia implies that the WNPH develops northward more than in the high AAO years. To examine this WNPH feature, this study analyzes 5,875 gpm contour, which can be defined as

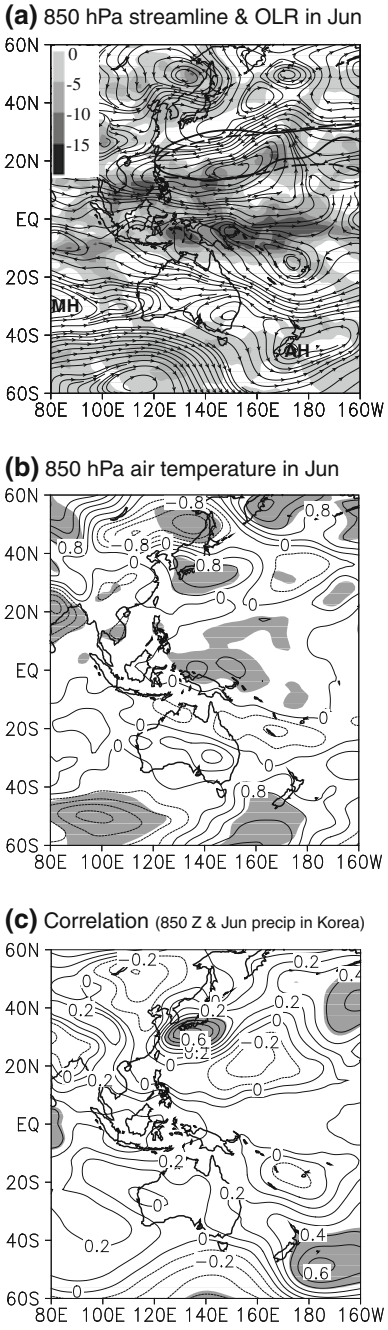

Fig. 9 Differences in (**a**) the 850-hPa streamline with OLR (*shaded*) and (**b**) 850-hPa air temperature in June between high AAO years and low AAO years and (**c**) the correlation distribution between 850-hPa geopotential height and June precipitation in Korea. In (**a**), *solid* and *dashed lines* denote 5,875 gpm contours for high AAO years and for low AAO years, respectively. *MH* Mascarene high, *AH* Australian high. Contour intervals are 5 W m^{-2} for OLR, 4°C for air temperature, and 0.1 for correlation distribution. Shaded areas in (**b**) and (**c**) denote regions >95% confidence level

the western periphery of the WNPH for the two phases. As mentioned above, the WNPH in the high AAO years develops more northward. As a result, the southwesterly is strengthened in Korea showing a low OLR (development

of convection) due to this feature of the WNPH. On the other hand, the meridional movement of the WNPH is generally related to the meridional movement of the summer rain band in the EASM region, as discussed above. Therefore, the Changma onset in the high AAO years is advanced more than in the low AAO years due to the WNPH northward being intensified in the high AAO years.

In the SH, the anomalous anticyclonic circulation is zonally intensified from the sea west of Australia to the region around New Zealand; in its north, the anomalous cyclonic circulation is located zonally. This is a typical characteristic of the positive AAO phase as shown by Gong and Wang (1999) and Thompson and Wallace (2000). The northerly from the anomalous anticyclone located to the west of Australia moves toward India, and the northerly from the anomalous anticyclone centered around New Zealand crosses the equator (cross-equatorial flow) and then converges with the westerly intensified in the tropical WNP. For the difference in the 850-hPa air temperature between the two phases, the negative value (cold air temperature) is located along the latter northerly (Fig. 9b). This negative value extends to 20°N. The two anomalous anticyclones centered in the sea west of Australia and the region around New Zealand are called as Mascarene high (MH) and AH, respectively (Xue et al. 2004). Previous studies have shown that MH is a main factor for the Indian summer monsoon (Krishnamurti and Bhalme 1976; Ramaswamy and Pareek 1978; Rodwell 1997). AH also causes strong cold outbreaks around Australia during the EASM onset period and then intensifies the cross-equatorial flow in the western Pacific; this cross-equatorial flow develops the WNPH northward again and the WNPH eventually causes to the rain belt to go northward. Many previous studies have shown that AH plays a decisive role in the variation of the EASM onset and EASM rainfall (Tao et al. 1983; Xue et al. 2004).

To clearly examine the relation between the June precipitation in Korea and AH, this study analyzes the one-point simultaneous correlation between the precipitation and 850-hPa geopotential height in June (Fig. 9c). Overall, the correlation distribution is similar to the spatial distribution of the difference between the two phases for the 850-hPa streamline. A positive correlation of over 0.5 at the 99% confidence level appears to the south of Korea and around New Zealand. As indicated above, the two high correlation areas are related to WNPH and AH, respectively. This implies that when a WNPH is intensified with an AH in June, the precipitation in Korea increases. There also exists a positive correlation in the MH region (sea west of Australia), although it is weak (not statistically significant). The correlation distribution between the two variables shows a similar result for the one-point simultaneous correlation analysis between the Changma onset date and 850 hPa geopotential height in June (not shown).

To understand the difference in the meridional vertical atmospheric structure for the longitude band (125°–130°E) of Korea between the two phases, this study analyzes the vertical cross-section averaged along 125°–130°E for the meridional circulation, vertical velocity, air temperature, and specific humidity (Fig. 10). The upward flow in low

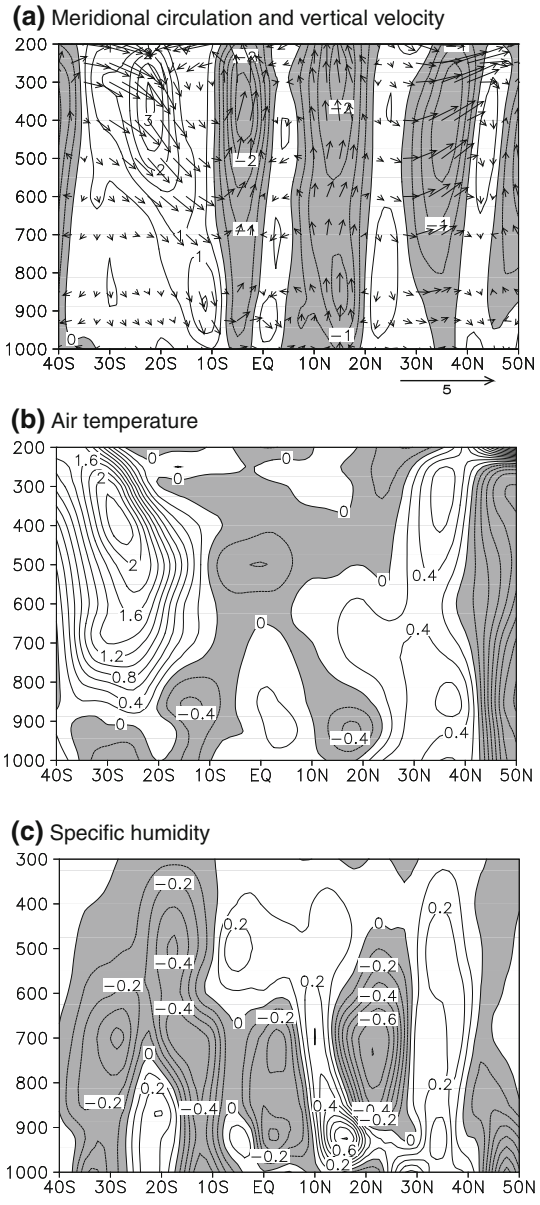

Fig. 10 Composite differences of latitude-pressure cross-section of (**a**) meridional circulations (vectors) and vertical velocity (contours), (**b**) air temperature, and (**c**) specific humidity averaged along 125°–130°E between high AAO years and low AAO years in June. The values of vertical velocity are multiplied by −100. *Shaded areas* denote negative values. Contour intervals are 0.5 hPa s^{-1} for vertical velocity, 0.2°C for air temperature, and 0.1 g kg^{-1} for specific humidity

latitudes (5°–20°N), downward flow in subtropics (20°–30°N), and upward flow in the mid-latitudes (30°–40°N), which is where Korea are located, are intensified in the high AAO years. In particular, warm and humid air is also intensified all over the troposphere with the intensified upward flow in the latitude band for Korea (Fig 10b, c); this atmospheric condition is more favorable for precipitation formation and an early Changma onset.

The downward flow is intensified through all of the levels in the low and mid-latitudes (10°S–40°S) of the SH for the high AAO years (Fig. 10a). In addition, a stable atmospheric structure with cold air temperature in the lower levels and warm air temperature in the upper levels is formed in this latitude band (Fig. 10b), and a dry state is intensified through all of the levels (Fig. 10c). These characteristics indicate that MH and AH are intensified in this latitude band during the high AAO years.

5.4 Tropical cyclone (TC) frequency around Korea

The role of the tropical cyclone (TC) in the variation of the June precipitation cannot be overlooked. Therefore, this study analyzes the tacks of TCs occurring in June for two phases (Fig. 11). Twelve TCs occur in June during the high AAO years, while five TCs do so during the low AAO years. This indicates that on average, two TCs occur each June during the high AAO years and one during the low AAO years. Moreover, more TCs land in Korea in June during the high AAO years (high AAO years: 4 TCs, low AAO years: 1 TC). This implies that TCs landing in Korea in June during the high AAO years play an important role in the increase in precipitation.

In general, TCs tend to move along the western periphery of the WNPH. As described above, the WNPH developed more northward during the high AAO years. This can be an important cause for more TCs landing in Korea in June during this phase.

6 Relation with AAO in the preceding March

Many previous studies showed that the signals of the variation in the EASM onset and precipitation can be identified through the characteristics of the preceding boreal spring AAO (Gao et al. 2003; Xue et al. 2004; Wang and Fan 2005; Fan 2006; Sun et al. 2009). This study also examines the lag-correlation of AAO in March, April, and May with the June precipitation in Korea and the Changma onset date. Of the 3 months, March AAO has the highest correlation with the June precipitation in Korea and the Changma onset date (Fig. 12). This may be because March is the transition season from the winter (summer) to the spring (fall) in the NH (SH). The AAO in March and the June precipitation in Korea show a high correlation of 0.48 at the 95% confidence level. For the Changma onset date (Fig. 12b), a negative correlation of more than -0.5 is established at the 99% confidence level. This indicates that when the AAO in March is strong, the June precipitation in Korea increases, and the Changma onset is advanced.

To examine the characteristics of the large-scale atmospheric environments in March that influence the June precipitation in Korea and the Changma onset, this study analyzes the differences for the 850-hPa streamline in March between the two phases (Fig. 13a). Overall, the results are not too different from those for June, except that the anomalous anticyclone located in the WNP dose not develop westward. The WNPH (or South Asia high) in the high AAO years is still intensified westward and northward more than during the low AAO years, although WNPHs of the two phases are located at lower latitudes than those in June. Meanwhile, the MH and AH in the SH clearly appears, and the negative 850-hPa air temperature is located around New Zealand toward the equator, although being not the same as in June (Fig. 13b). To verify that the June precipitation in Korea is also related to AH and MH in March, this study analyzes the one point lag-correlation between the June precipitation in Korea and the 850-hPa

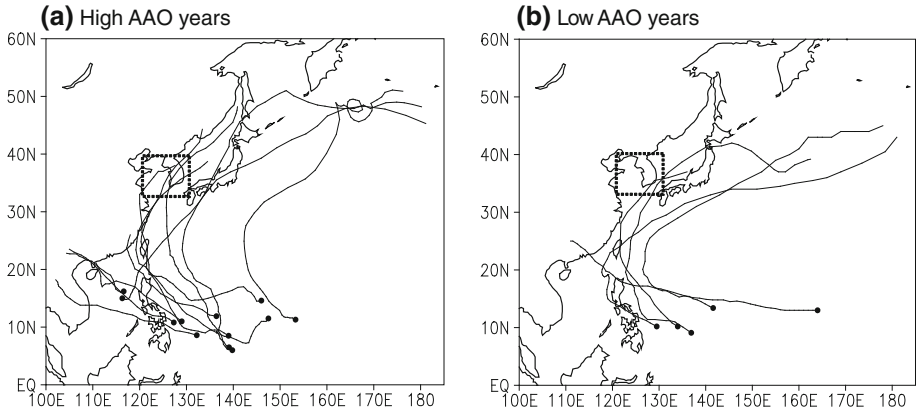

Fig. 11 Tracks of tropical cyclone in June during (**a**) the high AAO years and (**b**) the low AAO years. *Dotted boxes* denote Korea area

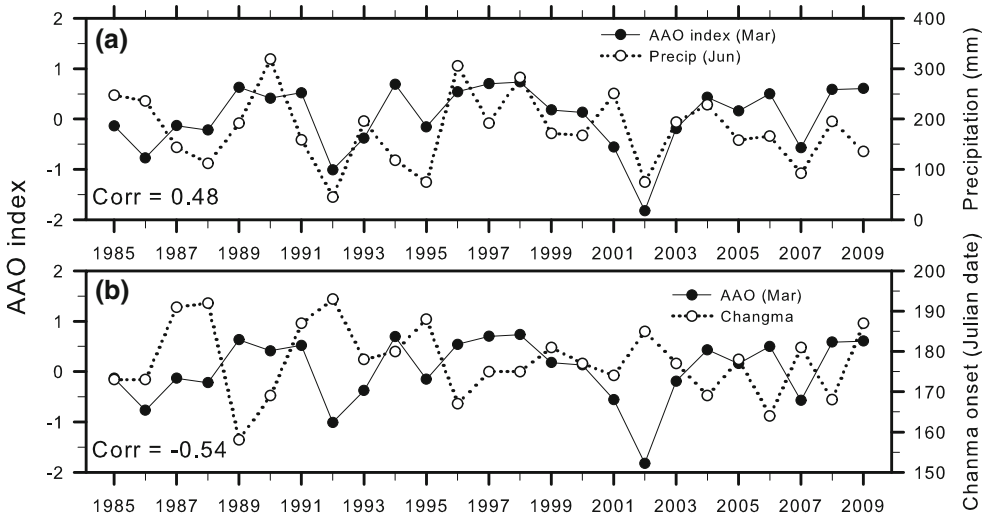

Fig. 12 Time series of AAO index in March, (**a**) June precipitation in Korea, and (**b**) Changma onset date

geopotential height in March (Fig. 13c). As analyzed above, the June precipitation in Korea and the Changma onset date had a strong correlation with AH relative to MH in June (Fig. 9c). The correlation distribution in March shows that June precipitation in Korea has a high correlation with MH more than AH, but the correlation with AH is not low. A similar correlation distribution is analyzed in the relation with the Changma onset (not shown).

7 Concluding remarks

This study defines the Changma onset in Korea using AWRI for the 25-year period (1985–2009). The onset is defined as the day the AWRI is over the average in June for the 25-year period. In addition, the days over the 25-year average AWRI should continue for more than 1 week after the onset, and the days with values under the average should not continue for more than 1 week after the onset. The 25-year average Changma onset date conforming to this definition is June 24 (standard deviation of 9 days). Afterwards, this study applies this definition to 60 weather observation stations over Korea and examines the spatial distribution of the 25-year average Changma onset date. Overall, the more northward a region is located, the later the Changma onset is.

To verify the validity of the Changma onset defined in this study, the correlation between AAO in June and the Changma onset date is analyzed. The AAO in June shows a high correlation with not only the Changma onset but also the June precipitation (AWRI) in Korea. This implies that when AAO in June is strong, the Changma begins earlier, which allows the June precipitation (AWRI) in Korea to increase. This feature is also shown through the correlation analysis of AAO with CMAP and OLR in June; the relation between them is most evident in Korea in northeast Asia.

To examine the cause of this correlation, this study defines five highest AAO years (high AAO years) and five lowest AAO years (low AAO years), excluding warm and cold ENSO years in the Niño-3.4 region during the total analysis period of 25 years; the differences between the averages of the former and the latter are analyzed with regard to various variables. The average Changma onset in the high AAO years is earlier by 10 days than in the low AAO years, and there is a difference of about 100 mm in precipitation. In AWRI, the moderate shortage of water resources only occurs for one of the high AAO years, while it occurs in three of the low AAO years. This indicates that abundant water resources are available for agricultural and industrial use in the high AAO years. More precipitation and higher AWRI in the high AAO years is clearly shown in the central area of the southern region and the western area of the northern region in Korea. For the spatial distribution of the Changma onset for the two phases, the Changma begins before June 19 in most regions for the high AAO years. For the low AAO years, the more northward a region is located, the later the Changma onset is. In particular, in the northwestern region in Korea, the Changma onset in the high AAO years differs by a maximum of 15 days from that in the low AAO years.

In the intraseasonal variation of the precipitation and AWRI, the largest difference between the two phases occurs in the summer. The precipitation and AWRI are more during Changma season before the second Changma season in the high AAO years and during the second Changma season in the low AAO years. For the variation in precipitation in the summer, there typically exist two peaks like the Changma and second Changma during the low AAO years but five peaks in the high AAO years. This may be because of the frequent heavy rainfall events during the high AAO years. Analysis results using CMAP data for the spatiotemporal variation of the 5-day average precipitation

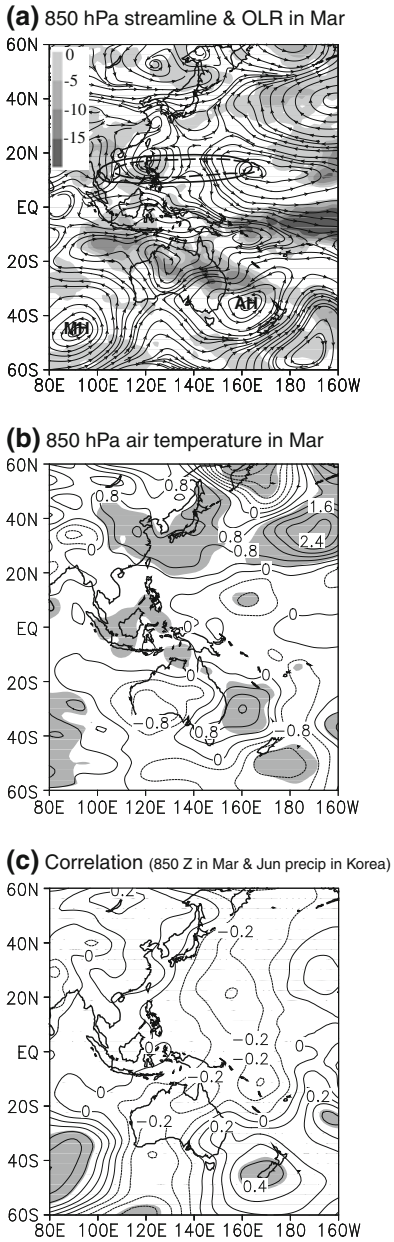

Fig. 13 Same as in Fig. 9, bur for difference in (**a**) the 850-hPa streamline with OLR (*shaded*) and (**b**) 850-hPa air temperature in March between high AAO years and low AAO years and (**c**) correlation distribution between 850-hPa geopotential height in March and June precipitation in Korea

in June reflects the early or late Changma onset dates well as defined using AWRI for the two phases.

Analysis of the difference in the large-scale atmospheric environments at 850-hPa level between the two phases shows that the June precipitation in Korea and the Changma onset are strongly related to the Mascarene high (MH) and Australian high (AH), which reflects the intensity of AAO in the SH well. In particular, AH causes strong cold outbreaks around Australia during the EASM onset period, intensifies the cross-equatorial flow in the western Pacific, and drives the WNPH to develop northward, which eventually plays an important role in moving the rain belt northward (Tao et al. 1983; Xue et al. 2004). This characteristic is also observed in the high AAO years. In addition, the June precipitation in Korea and Changma onset are highly correlated to two anomalous anticyclones in the preceding March. Therefore, this study suggests that the intensity of MH and AH in the SH in the preceding March may be used as a potential predictor for predicting the June precipitation in Korea and Changma onset.

A WNPH that develops more northward in June in the high AAO years is a major cause of more frequent landings of TCs in Korea; their frequent landings contribute considerably to increased June precipitation in Korea.

In this study, we focused on defining Changma onset in Korea using AWRI and verifying its validity. In our next study, we will (i) extend the target region for the definition of the Changma onset to the EASM, SCSSM, and Indian summer monsoon regions and verify its validity; (ii) define the Changma retreat in Korea using AWRI and analyze its validity; and (iii) examine in depth the relation of the Changma onset with ENSO, excluded in the present study.

Acknowledgments We would like to thank anonymous reviewers for their constructive and critical comments.

References

Byun HR, Lee DK (2002) Defining three rainy seasons and hydrological summer monsoon in Korea using available water resources index. J Meteorl Soc Jpn 80:33–44

Byun HR, Lee DK, Joung CH (1992) A study on the atmospheric circulation during the Dry Period before the Changma. Part I: existence and characteristics. Asia-Pacific J Atoms Sci 28:71–88 (In Korean with English abstract)

Chang HJ, Kwon WT (2007) Spatial variations of summer precipitation trends in South Korea, 1973–2005. Environ Res Lett 2:045012

Chang CP, Zhang Y, Li T (2000) Interannual and interdecadal variations of the East Asian summer monsoon and tropical Pacific SSTs. Part I: roles of the subtropical ridge. J Clim 13:4310–4325

Choi YJ (2004) Trends on temperature and precipitation extreme events in Korea. J Korean Geogr Soc 39:711–721 (In Korean)

Choi KS, Byun HR (2007) Definition of the onset and withdrawal of the Warm Season over East Asia and their Characteristics. Asia-Pacific J Atmos Sci 43:143–159

Ding YH (1992) Summer monsoon rainfalls in China. J Meteorol Soc Jpn 70:373–396

Fan K (2006) Atmospheric circulation in Southern Hemisphere and summer rainfall over Yangtze River valley. Chin J Geophys 49:672–679

Fan K, Wang HJ (2004) Antarctic oscillation and the dust weather frequency in North China. Geophys Res Lett 31. doi: 10.1029/2004GL019465

Gao H, Xue F, Wang HJ (2003) Influence of interannual variability of Antarctic oscillation on Mei-yu along the Yangtze and Huaihe

River valley and its importance to prediction. Chin Sci Bull 48:61–67
Gong DY, Ho CH (2003) Arctic oscillation signals in the East Asian summer monsoon. J Geophys Res 108(D2). doi:10.1029/2002JD002193
Gong DY, Wang SW (1999) Definition of antarctic oscillation index. Geophys Res Lett 26:459–462
Ha KJ, Yun KS, Jhun JG, Park CK (2005) Definition of Onset/Retreat and Intensity of Changma during the Boreal Summer Monsoon Season. Asia-Pacific J Atmos Sci 41:927–942 (In Korean with English abstract)
Hall A, Visbeck M (2002) Synchronous variability in the Southern Hemisphere atmosphere, sea ice, and ocean resulting from the annular mode. J Clim 15:3043–3057
Hendon H, Liebmann B (1990) A composite study of onset of the Australian summer monsoon. J Atmos Sci 47:2227–2240
Hendon HH, Thompson DWJ, Wheeler MC (2007) Australian rainfall and surface temperature variations associated with the Southern Hemisphere annular mode. J Clim 20:2452–2467
Ho CH, Kim JH, Kim HS, Sui CH, Gong DY (2005) Possible influence of the Antarctic Oscillation on tropical cyclone activity in the western North Pacific. J Geophys Res 110(D19104). doi:10.1029/2005JD005766
Huang RH, Wu YF (1989) The influence of ENSO on the summer climate change in China and its mechanism. Adv Atmos Sci 6:21–32
Inoue T, Matsumoto J (2003) Seasonal and secular variations of sunshine duration and natural seasons in Japan. Int J Climatol 23:1219–1234
Inoue T, Matsumoto J (2007) Abrupt Climate Changes Observed in Late August over Central Japan between 1983 and 1984. J Clim 20:4957–4967
Ju JH, Lu JM, Cao J, Ren JH (2005) Possible impacts of the arctic oscillation on the interdecadal variation of summer monsoon rainfall in East Asia. Adv Atmos Sci 22:39–48
Kalnay E et al (1996) The NCEP/NCAR 40-year reanalysis project. Bull Am Meteorol Soc 77:437–471
Kidson JW (1988) Interannual variations in the Southern Hemisphere circulation. J Clim 1:1177–1198
Kim KM (1979) A study on the rainfall characteristics of the rainy season in Korea. Asia-Pacific J Atmos Sci 15:55–70 (In Korean with English abstract)
Kim JW, Lee JG (2007) A qualitative analysis of WRF simulation results of typhoon 'Rusa' case. Atmosphere 17:393–405 (In Korean with English abstract)
Kim SS, Park SU, Lee BS (1983) The characteristics structural differences of the rainy front (Changma front) between the wet and dry seasons. Asia-Pacific J Atmos Sci 19:12–32 (In Korean with English abstract)
Kistler R et al (2001) The NCEP/NCAR 50-year reanalysis. Bull Am Meteorol Soc 82:247–267
Korea Meteorological Administration (1996) Changma white book. Korea Meteorological Administration, p 233
Krishnamurti TN, Bhalme HN (1976) Oscillation of a monsoon system, part I: observational aspects. J Atmos Sci 33:1937–1954
Kwok R, Comiso JC (2002) Spatial patterns of variability in Antarctic surface temperature: connections to the Southern Hemisphere Annular Mode and the Southern Oscillation. Geophys Res Lett 29. doi:10.1029/2002GL015415
Lau KM, Li MT (1984) The monsoon of East Asia and its global associations. Bull Am Meteorol Soc 65:114–125
Lau KM, Yang GJ, Shen SH (1988) Seasonal and intraseasonal climatology of summer monsoon rainfall over East Asia. Mon Weather Rev 116:18–37
Liang XZ, Wang WC (1998) Association between China monsoon rainfall and tropospheric jets. Q J R Meteorol Soc 124:2597–2623
Liebmann B, Smith CA (1996) Description of a complete (interpolated) outgoing longwave radiation dataset. Bull Am Meteorol Soc 77:1275–1277
Ramaswamy C, Pareek RS (1978) The southwest monsoon over Indian and its teleconnections with the middle and upper tropospheric flow patterns over the Southern Hemisphere. Tellus 30:126–135
Reason CJC, Rouault M (2005) Links between the Antarctic Oscillation and winter rainfall over western South Africa. Geophys Res Lett 32. doi:10.1029/2005GL022419
Rodwell MJ (1997) Breaks in the Asian monsoon: the influence of Southern Hemisphere weather systems. J Atmos Sci 54:2597–2611. doi:10.1029/2005GL022419
Sato N, Takahashi M (2001) Long-term variations of the Baiu frontal zone and midsummer weather in Japan. J Meteorl Soc Jpn 79:759–770
Seo KH, Lee DK (1996) Analysis and simulation of orographic rain in the middle part of the Korean Peninsula. Asia-Pacific J Atmos Sci 32:511–533 (In Korean with English abstract)
Silvestri GE, Vera CS (2003) Antarctic Oscillation signal on precipitation anomalies over southeastern South America. Geophys Res Lett 30: doi:10.1029/2003GL018277
Sun JQ, Wang HJ, Yuan W (2009) A possible mechanism for the co-variability of the boreal spring Antarctic Oscillation and the Yangtze River valley summer rainfall. Int J Climatol 29:1276–1284
Tao SY, Chen L (1987) A review of recent research on the East Asian summer monsoon in China. In: Chang C-P, Krishnamurti TN (eds) Monsoon Meteorology. Oxford University Press, Oxford, pp 60–92
Tao SY, He SX, Yang ZF (1983) An observational study on the onset of the summer monsoon over eastern Asia in 1979. Sci Atmos Sin 7:347–355 (in Chinese)
Thompson DWJ, Wallace JM (2000) Annular modes in the extratropical circulation, part I: month-to-month variability. J Clim 13:1000–1016
Wang HJ, Fan K (2005) Central-north China precipitation as reconstructed from the Qing dynasty: Signal of the Antarctic atmospheric oscillation. Geophys Res Lett 32. doi:10.1029/2005GL024562
Wang HJ, Fan K (2007) Relationship between the Antarctic oscillation and the western North Pacific typhoon frequency. Chin Sci Bull 52:561–565
Wang B, Lin Ho (2002) Rainy season of the Asian-Pacific summer monsoon. J Clim 15:386–398
Wang B, Lin Ho, Zhang YS, Lu MM (2004) Definition of South China Sea monsoon onset and commencement of the East Asia summer monsoon. J Clim 17:699–710
Xie P, Arkin PA (1997) Global precipitation: a 17-year monthly analysis based on gauge observation, satellite estimates, and numerical model outputs. Bull Am Meteorol Soc 78:2539–2558
Xue F, Wang HJ, He JH (2004) Interannual variability of Mascarene high and Australian high and their influences on East Asian Summer Monsoon. J Meteorol Soc Jpn 82:1173–1186
Yeh DZ, Tao SY, Li MC (1959) The abrupt change of circulation over the northern hemisphere during June and October. In: Bolin B (ed) The atmosphere and the sea in motion. Rockefeller Institute Press, New York, pp 249–267